Int. J. Appl. Math. Comput. Sci., 2023, Vol. 33, No. 2, 183–195
DOI: 10.34768/amcs-2023-0014

A DYNAMIC MODEL AS A TOOL FOR DESIGN AND OPTIMIZATION OF PROPULSION SYSTEMS OF TRANSPORT MEANS

GRZEGORZ PERUŃ [a]

[a] Faculty of Transport and Aviation Engineering
Silesian University of Technology
ul. Krasińskiego 8, 40-019 Katowice, Poland
e-mail: grzegorz.perun@polsl.pl

Designing power transmission systems is a complex and often time-consuming problem. In this task, various computational tools make it possible to speed up the process and verify a great many different solutions before the final one is developed. It is widely possible today to conduct computer simulations of the operation of various devices before the first physical prototype is built. The article presents an example of a dynamic model of power transmission systems, which has been developed to support work aimed at designing new and optimizing existing systems of that type, as well as to help diagnose them by designing diagnostic algorithms sensitive to early stages of damage development. The paper also presents sample results of tests conducted with the model, used at the gear design stage. In the presented model, the main goal is to reproduce the phenomena occurring in gears as well as possible, using numerous experiments in this direction featured in the literature. Many already historical models present different ways of modeling, but they often made significant simplifications, required by the limitations of the nature of computational capabilities. Differences also result from the purpose of the models being developed, and the analysis of these different ways of doing things makes it possible to choose the most appropriate approach.

Keywords: dynamic model, gear, power transmission system, optimization, diagnostics.

1. Introduction

The vibroacoustic activity of gears, which are classified as complex nonlinear mechanical vibration generators, has been the target of research at many scientific and research centers for years. Gears are one of the most basic devices used in the construction of various machines, especially since they are part of their power transmission systems, also currently in high-speed trains (Cheng *et al.*, 2022). The need to change speed with a simultaneous change of the torque has accompanied human activity almost forever, especially since the industrial revolution.

Since the development of the first dynamic models of gears, the software has also developed significantly, which makes the processing of numerical models significantly easier and faster. It is no longer necessary to develop algorithms for solving the equations, as this has been taken over by appropriate simulation environments, which allows focusing attention on the most important task, i.e., preparing the equations of the model itself. It invariably requires expert knowledge to take into account all relevant factors that affect the course of the analyzed phenomena, experience from observations of the modeled devices, and the resulting ability to simplify the algorithms from factors that do not affect the studied phenomenon or this influence is negligibly small and would unnecessarily complicate the construction of the model.

The diversity of power transmission systems and their application do not allow the creation of a single procedure for the design of such structures, and thus a universal tool that all designers could use. However, it is possible to develop a set of tools in a specific computational environment that will significantly simplify the process of designing new structures or optimizing existing ones. In addition, with the use of the same tool, it will become possible to diagnose such systems by conducting simulations of various combinations of malfunctions.

At the current stage of the presented work, it is possible to simulate the operation of fixed-axis gears in a power transmission system, which also consists of couplings, an electric motor, drive shafts, and a working machine. The degree of development of these components varies; moreover, for example, the motor model comes in two varieties, significantly differing in the accuracy of the description of the processes taking place. Regardless of the purpose of the calculations carried out, models of gears that describe the work in great detail are used. Based on these models the concept of gear mesh description developed by Müller and published in numerous works was adopted. The correspondingly expanded concept now makes it possible to take into account a much larger number of factors and use it in a wide range of possible research.

Because models allow obtaining results consistent with those of measurements on real objects, the use of dynamic modeling makes it possible to determine the influence of all factors of interest on dynamic phenomena, which is not always possible even under laboratory conditions due to the economic factor, among other things (Piskur *et al.*, 2021; Grzadziela *et al.*, 2021). This is the main direction already indicated, in which dynamic models are quite widely used, both at the stage of construction and later to optimize already existing structures. The computational results obtained from such models can also be used in other tools, albeit in FEM environments (Grzadziela *et al.*, 2022). Results from the model presented below can be taken also as input data—the forces acting on the body of the gearbox to search for its optimal shape.

In this context, many potential opportunities for the use of dynamic gear models can be noted—the design of gears with a high ratio of power transmitted by the gears to their mass, reduction of the nominal load on the teeth by increasing the speed of the wheels, minimization of vibration, emitted noise, maximization of service life, etc. At this stage, it is quite easy to encounter a situation where meeting one criterion causes difficulties in meeting another, so it is necessary to work out some compromise.

The second significantly different direction, which was also pointed out earlier, is the generation, with the model, of waveforms of quantities that can carry information about the technical condition of the device. By simulating local damage, it is possible to obtain signals that, when processed appropriately, can provide information about the need for a condition check. In addition, carrying out multiple simulations of different defects, including those occurring simultaneously, can also provide information not only about the appearance of the problem, but also about the source of the problem.

The article presents a developed dynamic model of a gearbox operating in a circulating power system, conditions for validating the model on real objects, and an example of using the model. The model was developed mainly for research aimed at designing new and optimizing existing gears and power transmission systems, as well as to assist in diagnosing them by designing diagnostic algorithms sensitive to the early stages of damage development. As an example of the model's application, the paper presents sample results of calculations carried out using it, aimed at optimizing the construction of gears at the design stage.

2. Short review of dynamic models of gears and power transmission systems with gears presented in the literature

Ajmi and Velex (2005) note that numerous gear models have been proposed in recent decades, ranging from dynamic models with one degree of freedom to elaborate three-dimensional finite element ones. A vast majority of simulations to date are based on rigid-body lumped parameter models with the mating teeth assimilated to lumped stiffnesses. A detailed review of historical gear dynamics models with vibration emphasis can be found in the review papers by Blankenship and Singh (1992), Özgüven and Houser (1988), Wang *et al.* (2003), and Bartelmus (2001).

In the literature, different approaches to the modeling of gears can be found. Not only dynamic models are developed, but analytical ones, among others, as well. Such a model of the gear mesh in a three-dimensional version is described by Neusser *et al.* (2017), noting that it is a tool that allows one to model gear noise emissions such as gears rattling, hammering and whining, and to more accurately predict gears errors. In another paper (Choy *et al.*, 1996), an analytical model was developed to analyze wear and pitting on working surfaces simulated through changes in the amplitude and phase of the mesh stiffness.

A nonlinear dynamic model of spur gear transmissions that takes into account both relief and manufacture errors in the tooth profile is presented by Fernández *et al.* (2014). It allows dynamic analysis of a gear transmission supported by ball bearings. To study the interaction between the surface wear and the gear dynamic response, dynamic models and an FEM model were used by Ding and Kahraman (2007). A dynamic gear wear model was proposed which includes the influence of worn surface profiles on dynamic forces in meshing and transmission errors as well as the influence of dynamic tooth forces on wear profiles.

The lumped parameter model developed to study the dynamic behavior of a two-stage straight bevel gear system is presented by Yassine *et al.* (2014). The article also presents a method for modeling interlocking stiffness, tooth deflections, and manufacturing defects.

Dynamic simulations of helical gears and wide-faced spur and helical gears with the use of a 3D dynamic model is the subject of the work of Osman and Velex (2010). The paper by Alves *et al.* (2012) synthesizes all the work carried out on spiral bevel gears from the point of view of quasi-static and dynamic models. Two three-dimensional dynamic models with lumped parameters are presented.

Mohammed *et al*. (2015) presented a dynamic model of a 12 DOF spur gear for vibration-based simulation and condition monitoring. The modeling of a spur gear with friction and cracks is described by Howard *et al*. (2001). The modeling of damage by appropriately changing the stiffness of the gear mesh is also shown by Pandya and Parey (2013) or Ma *et al*. (2015).

In the work of Chen *et al*. (2017), two analytical computational models of gear mesh stiffness were proposed for spur gears with a crack of the tooth root. Also, a model for damage diagnosis was addressed by Dadon *et al*. (2018). It combines the most advanced approaches to modeling the contact between pairs of gears as a set of springs, modeling the effect of damage on mesh stiffness, and integrating geometric errors.

Dynamic models of planetary gears have also been developed for years. For the study of a planetary gear having manufacturing errors, to predict modulation sideband, a nonlinear time-varying dynamic model was proposed by Inalpolat and Kahraman (2010). Other studies aimed at the effect of torque on the dynamic behavior and system parameters of planetary gears, largely based on a measurement experiment, presented by Ericson and Parker (2014), also extensively discuss various models, including analytical and dynamic ones of this type gears. They are the subject of the author's previous work (Peruń, 2006; 2017). The planetary gear dynamic model is also presented by Gu and Velex (2013) for dynamic simulation of eccentricity errors. Despite the limited number of degrees of freedom, complex effects were obtained in instantaneous rigid-body motions, couplings between errors, DOF interactions and gear geometry, and modulated mesh stiffness functions. In the work of Lai *et al*. (2022), a Ravigneaux planetary gear system with an unloaded floating ring gear was studied. A rigid dynamic model and three-dimensional dynamic loading of the planet gears are presented. Modeling vibration signals of a planetary gearbox in a proper technical state and with the cracked tooth is described by Liang *et al*. (2015).

3. Dynamic phenomena occurring in gears

To develop a tool to facilitate the process of designing gears, as well as their subsequent diagnosis, it is necessary to understand the phenomena occurring in these machines. There are many sources of dynamic phenomena in them, causing vibration and noise. The first presented goal of model development included optimization of new and existing gear designs, so the overriding goal is to select their parameters so that they not only meet the objectives, but also their operation is characterized by specific parameters. The second goal posed to the models in this work is to use these side phenomena to determine the technical condition of these devices. The signals generated, for example, vibration velocities in different technical states, can be used to look for symptoms of simulated malfunctions, and thus to develop diagnostic algorithms for existing gear designs. In both of these issues, it is important to know the nature of the phenomena occurring in gears and to be able to analyze them accordingly.

Phenomena occurring in gears, and thus to some extent transferred to other components of the power transmission system, have their origin both in the gear itself and in the interaction of other components of the power transmission system with the operation of the gear. For this reason, they can be divided into internal, resulting from the realization of the function of the target, and therefore caused by the interaction of wheel gears, the interaction of bearings, the dynamic response of the gear body, and external, resulting from mechanical excitations caused by the work of other elements, and causing torque and speed disturbances.

Internal sources constitute the largest group of factors and are shaped already at the design stage. The following are related to the proper operation of gears: the entry into the mesh of pairs of teeth and the resulting impact of teeth, changes in the stiffness of teeth at the meshing section, and changes in the frictional force due to inter-tooth slips. Lower grades of gear accuracy cause the appearance of significant deviations in pitch, outline, and tooth line, which is the reason for the increase in dynamic excess. Due to the occurrence of wear and the appearance of damage, the first group can be expanded to include further sources, like inadequate lubrication; similarly, in the second group, assembly errors and unbalance, among others, can be added. All of these factors together are responsible for overall vibration and noise levels, and for this reason, it is now advisable to develop dynamic models that also allow these phenomena to be analyzed together. This makes it possible to more fully shape vibroactivity already at the design stage, and, with a more faithful description, the diagnostic algorithms created will be characterized by better efficiency.

With the goal of minimizing the vibroactivity of the gear or the entire power transmission system, it is also convenient to divide the sources of these phenomena into those related to the design, the technology of manufacture, as well as to the operating conditions. Minimizing vibroacoustic activity without considering the relationship between these factors is not possible, or at least not as effective.

In an ideal single-stage gear with parallel axes, the vibroacoustic signal contains only the mesh frequency and its harmonics. In real gears, the power of the vibroacoustic signal is contained mainly in the band of the mesh frequency, and, due to the presence of an involute error, also in the bands of its initial harmonics. In addition, there are rotational frequencies of the shafts and their harmonics, resulting, among other things, from eccentric seating or wheel unbalance. These can be seen in the low-frequency part of the spectrum as well as in the form of sidebands formed from the modulation of the meshing frequency and its harmonics. In addition to the above-mentioned spectral components, gears are affected by some design and operational factors that force vibrations, which can modulate the amplitude and frequency of the signal generated in the gearing. To be mentioned here are pitch deviations, wear of working surfaces, and local damage to teeth. The rolling bearings are also an additional source of modulation. The causes of vibration generated by the bearing can be divided into structural, manufacturing, and operational.

In planetary gears, the structure of the spectrum is more complicated than that known from ordinary fixed-axis gears. In the spectrum, there are additional components with characteristic frequencies, which include the frequencies of entry into the tooth mesh of the sun wheel, those of entry into the tooth mesh of the internally toothed wheel, and the ones of entry into the tooth mesh of a planetary wheel. They are directly related to the design of the planetary gear. From the point of view of the correct operation of planetary gears, it is essential to ensure that the load is distributed evenly over the individual planets.

The dynamic interaction in the mesh zone modulated by the series-connected interaction of the rolling bearings induces vibration of the gear body. The body is characterized by a complex resonant structure and is the main emitter of noise. The combination of the signal coming from the mesh and the transition function from the source to the receiving point is the basis for evaluating the vibroacoustic activity of gears.

Whatever the sources of dynamic phenomena are, they cause vibration and noise during operation, which is not favorably perceived from the point of view of comfort and work evaluation. It is desirable to reduce these residual phenomena to a minimum, which can be achieved by the appropriate shaping of vibroactivity at the source itself—in the gear mesh, as well as on their propagation path, in the final stage by the appropriate shaping of the body, which is the main emitter of noise. Reducing vibroacoustic phenomena also makes it possible to influence the time of failure-free operation. Therefore, the developed model can be a valuable design tool to facilitate the development of gears with the desired design, performance, and durability parameters.

4. Modeling dynamic phenomena in gears

The previous sections focused on the presentation of gear models shown in the literature and the phenomena occurring in gears. This part begins with a description of the developed model and how it takes into account a selection of the most important factors. The adopted method of describing the various phenomena was taken from the literature on modeling gears (e.g., Dabrowski *et al.*, 2000) and works that deal with the analysis of the phenomena occurring in gears. In addition, the results of ongoing experimental research on test stands with gears operating in a circulating power system were used.

By dividing the factors affecting the operation of gears into groups related to design, manufacturing technology, and operating conditions, it was possible to determine the functionalities necessary in the model. As mentioned earlier, due to the purpose of the models, the phenomena occurring in the gears were described in some detail. Among the structural factors, in addition to the obvious parameters such as the number of teeth and modulus, the width of the wheels, the transverse pressure angle, circumferential clearance, variable mesh stiffness and vibration damping in the mesh, the values of the transverse and face contact ratios, as well as the presence and parameters of modification of the tooth outline and tooth line, among others, were taken into account. It is also possible to enter information on the wear of tooth working surfaces in a simplified manner. Although many older models were developed assuming a constant stiffness of a pair of teeth along the meshing section and such simplification is now too much and it is necessary to determine the number of pairs of teeth located in the meshing section, the points of cooperation of each pair of teeth, and, on this basis, with the knowledge of the stiffness characteristics, the correct value of stiffness is determined.

The stiffness of a mesh is defined as the ratio of the force acting along a meshing section to the deflection of the teeth. Its value is influenced by the geometry of the mesh and material constants, including the modulus of elasticity. To determine the mesh stiffness of one pair of teeth, among the various methods presented in the literature, it was decided to use in the model the method from the research of Niemann and Baethge (Dabrowski *et al.*, 2000).

The method adopted allows to obtain stiffness values taking into account many geometric parameters such as the contact angles on the wheels' top diameters, the contact angle on the rolling diameter, the nominal contact angle, the basic and rolling diameters of the wheels, outline displacement coefficients, tooth numbers, or modulus, and also takes into account the elastic modulus of the material and Poisson's number. The total deformation of a pair of teeth w is determined by the sum of the deflection of the teeth under normal force taking into account the rim deformation, denoted for the pinion as w_1 and for the wheel as w_2, and the flattening of the tooth contact surface w_H.

The mesh stiffness c_{zaz}, the deformation of a pair of teeth w and the unit load Q are connected by the relation

$$c_{zaz} = \frac{Qd_{w1}}{w}, \tag{1}$$

where c_{zaz} is the mesh stiffness [N/(mm·µm)], Q is the unit load [MPa], d_{w1} is the rolling diameter of the pinion [mm], w is the total deformation of a pair of teeth [µm].

Given the number of data items included in the calculations, and the correspondence between the results of the calculations and the experimental results presented in the literature, the method was considered suitable for application. It sufficiently reflects reality and eliminates the biggest possible simplification—a constant stiffness value, and, additionally, was easy for adapting to the developed model. Also bearing in mind the need to ensure the possibility of simulating the operation of gears, for example, with helical gears or with various modifications, all the necessary calculations are carried out not only along the meshing section, but also along the width of the gear, which makes it possible to simulate the operation of gears with different geometries and parameters. The stiffness of a pair of teeth is determined for a selected number of tooth contact points uniformly distributed along the meshing section. The accuracy of the stiffness characteristics is determined by the assumed number of points per base pitch, where the guiding calculations are carried out. The stiffness characteristics of the tooth pair are then approximated by a third-degree polynomial, the coefficients of which are the input data for simulation calculations.

The stiffness characteristics taken into account in the study are determined based on the assumed, mainly geometric data of the gears. At the stage of research presented in the article, the source of this data was the actual gears of the FZG stands on which model verification took place.

To correctly describe the phenomena occurring in the gear mesh, it is also necessary to introduce vibration damping in the mesh into the model. Damping in the gear results from the damping properties of the materials used to manufacture its components and many phenomena occurring during its operation, such as energy dissipation in the oil layer between the teeth, the friction of the tooth surfaces, or in the bearings and the splashing of oil causing power losses. For numerical calculations the literature recommends selecting damping coefficients in such a way that the results are consistent with experience at least for resonant states, in the simplest case, assuming a linear dependence of the damping force on the speed of vibration (viscoelastic damping).

The damping of vibrations in the gears was modeled using the dimensionless damping coefficient specified by the relation

$$k_z = a_t + b_t v + c_t v^2 + d_t v^3, \tag{2}$$

where k_z is the dimensionless damping coefficient, a_t, b_t, c_t, d_t are dimensionless coefficients of polynomial damping, v is the linear velocity of mesh in m/s.

If the determined value is less than 0.1, which corresponds to velocities v greater than about 30 [m/s], a value equal to 0.1 is used for further calculations.

The losses caused by splashing oil through the gear wheel are described by a dimensionless loss factor calculated from the formula

$$s_o = \frac{v^p bH\sqrt{v_o}}{100000rN}, \tag{3}$$

where s_o is the dimensionless loss factor, v is the linear velocity of mesh [m/s], b is the width of the wheel [mm], H is the depth of immersion of the wheel in oil [mm], v_o is the kinematic viscosity of oil [mm^2/s], p, r are the dimensionless coefficients, N is the power transmitted by the gear [kW].

The vibroacoustic activity of gears is significantly determined by the accuracy of the manufacture and assembly of its components, i.e., factors related to the implementation of the technological process. Among these, the most common are deviations in the pitch of the teeth of the wheels, deviations in the outline and line of the teeth, including those caused by the deviation of the mesh angle, the condition, and roughness of the working surfaces of the teeth, wheel runout, and eccentricity, non-uniformity, eccentricity and deviation of the distance of the axles. The gear model takes directly into account all the mentioned factors except the roughness of the working surfaces of the teeth. By shaping the appendage surfaces, the model makes it possible to take into account periodic outline deviations, outline modifications, tooth line deviations, and modifications, as well as wear on the tooth working surfaces. The gears are modeled as elementary gears with straight teeth, and, in the case of helical gearing, they are shifted relative to each other in a phase that depends on the angle of inclination of the tooth line on the base diameter. It is possible to carry out dynamic calculations of gears with high teeth, characterized by a value of the spur gear ratio greater than 2 (HCR), not only the gear pairs with a low contact ratio (LCR). On the other hand, it was assumed that the minimum value of this ratio could be 1, and only locally, in the presence of tooth damage, correspondingly lower. Knowing the coordinates of the points of cooperation of the teeth on the meshing section allows the calculation of the stiffness of a single pair of teeth and also, among other things, the value of the deviation of the position of the outline and the depth of any tooth modification.

The force in the mesh transmitted by a single pair of teeth is the product of the total deflection of a pair of teeth and its stiffness, which varies along the meshing section. Its value can be different depending on that of simulated deviations and locale damage. A pitch deviation is assigned to each tooth, and the numbers of matching teeth are calculated in each simulation step individually in each gear. The algorithm makes it possible to simulate tooth pitch deviations, deviations in the tooth outline position, and the tooth line.

Among the operating factors, variable load, variable speed, operating temperature, and oil viscosity are included in the model.

Rolling bearings, whose rigidity is of the same order as that of the gear, can be used for bearing the shafts in the gear. For this reason, it seems appropriate to include their stiffness in the model as well, for which calculation methods are taken from the literature. They allow the determination of nonlinear characteristics of the displacement of the shaft in the direction of the force. The stiffness of the bearing can be expressed by the general relation

$$c_b = \frac{Q_{\max}(t)}{\delta_r(Q_{\max})}, \tag{4}$$

where c_b is the stiffness of the bearing [N/m], $Q_{\max}$ is the maximum load on the rolling part [N], δ_r is the radial displacement of the bearing journal [m], t is time.

In the case of an ordinary ball bearing, when only the values of the maximum load on the rolling part and the diameter of the rolling element are given, a numerical formula can be used to calculate the radial displacement of the journal:

$$\delta_r = \frac{0.44 Q_{\max}^{\frac{2}{3}}}{d_k^{\frac{1}{3}} \cos(\alpha)}, \tag{5}$$

where δ_r is the radial displacement of the bearing journal [μm], $Q_{\max}$ is the maximum load on the rolling part [N], d_k is the diameter of the rolling element [mm], α is bearing operating angle [rad].

When the number of rolling elements is known among the bearing parameters, the following formula can be used:

$$\delta_r = 0.96 \left(\frac{(\frac{R}{2e})^2}{0.1 d_k} \right)^{\frac{1}{3}}, \tag{6}$$

where δ_r is the radial displacement of the bearing journal [μm], R is the radial bearing load [N], e is the number of rolling elements in the bearing, d_k is the diameter of the rolling element [mm].

The corresponding numerical formulas for selected other bearing types can be found in the literature. Often, a change in the type of bearing corresponds to a change in the coefficient appearing in the formulas, e.g., for double-row self-aligning bearings, the value in the formula (6) will be changed from 0.44 to 0.70, while in the formula (7) the value of 0.96 will be replaced with 1.435.

A very simple relationship was used to determine the bearing friction torque:

$$M = 0.5 P d_m, \tag{7}$$

where M is the friction torque in bearing [Nm], μ is the constant coefficient of friction of the bearing, P is the equivalent dynamic load of the bearing [N], d_m is the average diameter of the bearing [m].

5. Characteristics of a dynamic model and equations of motion

This publication will present a method of modeling dynamic phenomena in a power transmission system using a circulating power gear bench system as an example. The choice of this modeling station was due to two main reasons: firstly, this station is used in a wide range of research, far beyond its primary application, and secondly, there was an opportunity for very fine tuning of the model and its validation. The development of the model was aimed at replacing selected studies conducted in the laboratory with numerical studies. In the literature, the results of analysis of various tests conducted using this stand can be found, including, for example, the FEM model presented by Razpotnik *et al.* (2015), which confirms its research utility. The stand was also used to compare the results of analytical and experimental studies of gear micropitting initiation and propagation under varying loading conditions (Al-Tubi *et al.*, 2015). The usefulness of the stand was also appreciated by Marques *et al.* (2016), who demonstrated a model and sample tests.

The model features two gears, an electric drive motor, coupling, bearings, and shafts. A diagram of the model is shown in Fig. 1.

Tests on the modeled bench can be carried out at both constant and variable speeds. The speed is changed through a frequency converter, through which an asynchronous motor is powered, whose main role is to compensate for power losses in the system. The load can be varied by changing the steering angle of the tension coupling. The closing gear and the test gear are characterized by equal gear ratios and axle spacing.

The developed model used two coordinate systems associated with each gear. The determinant of the directions of the axes of these systems was the direction of the inter-gear force, different in the two gears. Only the direction from both systems is identical, and it runs along the gear shafts. The x-axis points in the direction of the mesh force, while the y-axis points in the direction of the frictional force in the mesh. The described approach was intended to facilitate the description of the phenomena occurring in gears, but without eliminating their interaction with each other.

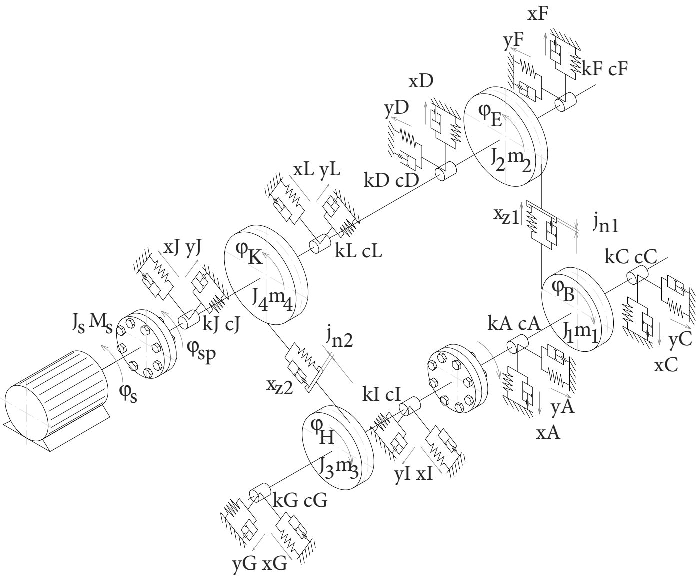

Fig. 1. Dynamic model of a station with gears operating in a circulating power system (S: electric motor; sp, wn: coupling; H and 3, B and 1: pinions; K and 4, E and 2: wheels; A, C, D, F: bearings of the test gear; G, I, J, L: bearings of closing gear; J: moments of inertia; M: torques; m: masses; c: stiffness; k: damping coefficients).

The equations of motion of the developed models were determined from the general relationship

$$\frac{\mathrm{d}}{\mathrm{d}_t}\left(\frac{\partial E_k}{\partial \dot{q}_i}\right) - \left(\frac{\partial E_k}{\partial q_i}\right) + \left(\frac{\partial E_p}{\partial q_i}\right) = Q_i - \frac{\partial D}{\partial \dot{q}_i}, \quad (8)$$

$i = 1, 2, \dots, n_{df}$, where E_k is the kinetic energy of the system, E_p is the potential energy of the system, Q_i are generalized forces, D is energy dissipation of the system, q_i are generalized coordinates, n_{df} is the number of degrees of freedom.

The coupling connecting the motor to the wheel shaft of the closing gear is described by an angular displacement with respect to the shaft axis (z):

$$\begin{aligned}\ddot{\phi}_{sp} J_{sp} &= c_{Ssp}(\phi_s - \phi_{sp}) + k_{Ssp}(\dot{\phi}_s - \dot{\phi}_{sp}) \\ &\quad - c_{spK}(\phi_{sp} - \phi_K) + k_{spK}(\dot{\phi}_{sp} - \dot{\phi}_K). \quad (9)\end{aligned}$$

The radial displacement of the bearing of the wheel shaft in the direction of the resultant (w) of the normal mesh force (acting in the direction of the x-axis) and the friction force in the mesh (acting in the direction of the y-axis is

$$\ddot{w} m = F - c(w)w - k\dot{w}, \quad (10)$$

where F is force in bearing.

The angular displacement of the pinion relative to the z-axis (closing gear) is

$$\begin{aligned}&\ddot{\phi}_H J_3 \\ &\quad = F_{z2}\cos\alpha_w r_{w3} + F_{t2}\sin\alpha_w r_{w3} \\ &\qquad - c_{Hwn}(\phi_H - \phi_{wn}) - k_{Hwn}(\dot{\phi}_H - \dot{\phi}_{wn}) \quad (11) \\ &\qquad + \dot{\phi}_H(k_{\phi G} + k_{\phi H} + k_{\phi I}) \\ &\qquad - M_{sG} - M_{sI},\end{aligned}$$

where F_{z2} is force in the meshing of the closing gear [N], F_{t2} is friction force in the meshing of the closing gear [N], M_{sJ}, M_{sL} are torques in bearings J and L [Nm].

The angular displacement of the wheel relative to the z-axis (closing gear) is

$$\begin{aligned}\ddot{\phi}_K J_4 = &-F_{z2}\cos\alpha_w r_{w4} - F_{t2}\sin\alpha_w r_{w4} \\ &+ c_{spK}(\phi_{sp} - \phi_K) + k_{spK}(\dot{\phi}_{sp} - \dot{\phi}_K) \\ &+ c_{EK}(\phi_E - \phi_K) + k_{EK}(\dot{\phi}_E - \dot{\phi}_K) \\ &- \dot{\phi}_K(k_{\phi_J} + k_{\phi_K} + k_{\phi_L}) - M_{sJ} - M_{sL}. \\ &\qquad (12)\end{aligned}$$

In much the same way as the phenomena in the closing gear and its bearings were modeled, as well as the coupling connecting the motor to the closing gear, the phenomena in the second gear of the stand and its other components were modeled.

The results of the simulation are the actual values of, among other things, displacements, velocities, and accelerations of individual elements from selected time intervals or from the entire calculation, the time profiles of mesh forces in each mesh, the profiles of forces transmitted by individual pairs of teeth (also in the form of spatial diagrams), as well as forces in bearings.

The inclusion in mathematical models of drive systems of a description of the dynamic phenomena occurring in the engine is due to their dynamic effects on the gear that transmits the drive. Regardless of the description adopted from the two alternative methods used, the basic set of parameters determined includes the angular displacement of the engine rotor and the driving torque. The rotor's moment of inertia and, in the extended version of the description, several electrical parameters are included in the calculations.

The simplified model of the drive motor is described by a single differential equation:

$$\ddot{\phi}_s = \frac{M_s(n_s) - M_n}{J_s}, \tag{13}$$

where $\ddot{\phi}_s$ is the rotor angular acceleration [rad/s^2], M_s is the motor torque determined from its mechanical characteristics [Nm], M_n is the load torque on the motor rotor [Nm], n_s is the rotor speed [rpm], J_s is the rotor moment of inertia [kg·m^2].

The advantages of this simple description are the low cost of calculations, the lack of need to identify electrical parameters (the model does not consider any electrical parameter, only mechanical), and the values of speed and torque required to determine the static mechanical characteristics, as well as the moment of inertia, which can be obtained from the manufacturer's catalog. Disadvantages from the point of view of the bench model and its assumed field of application include the failure to take into account the dynamic phenomena occurring during transient operation, which can significantly affect the operation of the power transmission system.

The use of this simplified description of engine operation, therefore, represents a certain compromise between calculation time and expectations of results. If, from the point of view of research, transients such as starting and braking of the stand are not of utilitarian importance, only the results obtained during steady-state operation are significant, then the use of this method of modeling is fully justified, and the results of calculations from the analyzed time of operation of the stand are correct and consistent with the results of measurements obtained on the test stand. However, if it is also necessary to analyze the operation of the gear, for example, during the start-up, it becomes necessary to take into account a more complex motor model. Hence the implementation of the model in two varieties.

During calculations with the use of a mechanical-electrical model, the instantaneous values of phase currents, magnetic fluxes, and winding voltages, among others, are also determined. For this purpose, a model in the $0dq$ orthogonal coordinate system, well-known in the literature, in which the stator and rotor axis systems are stationary for each other, and the stator and rotor windings are reduced to equivalent two-phase windings, is used. The choice of this coordinate system to describe a three-phase AC machine was due to the optimization of the simulation process time.

The electrical part of the motor description is represented by the equations (SPS, 2009)

$$V_{qs} = R_s i_{qs} + \frac{\mathrm{d}\phi_{qs}}{\mathrm{d}t} + \omega_e \phi_{\mathrm{ds}}, \tag{14}$$

$$\phi_{qs} = L_s i_{qs} + L_m i'_{qr}, \tag{15}$$

$$\phi_{\mathrm{ds}} = L_s i_{\mathrm{ds}} + L_m i'_{\mathrm{dr}}, \tag{16}$$

$$V_{\mathrm{ds}} = R_s i_{\mathrm{ds}} + \frac{\mathrm{d}\phi_{\mathrm{ds}}}{\mathrm{d}t} - \omega_e \phi_{qs}, \tag{17}$$

$$V'_{qr} = R'_r i'_{qr} + \frac{\mathrm{d}\phi'_{qr}}{\mathrm{d}t} + (\omega_e - \omega_r)\phi'_{\mathrm{d}r}, \tag{18}$$

$$\phi'_{qr} = L'_r i'_{qr} + L_m i_{qs}, \tag{19}$$

$$\phi'_{qr} = L'_r i'_{qr} + L_m i_{qs}, \tag{20}$$

$$V'_{dr} = R'_r i'_{dr} + \frac{\mathrm{d}\phi'_{dr}}{\mathrm{d}t} - (\omega_e - \omega_r)\phi'_{qr}, \tag{21}$$

$$L_s = L_{ls} + L_m, \tag{22}$$

$$L'_r = L'_{lr} + L_m, \tag{23}$$

$$T_e = 1.5p(\phi_{ds} i_{qs} - \phi_{qs} i_{ds}), \tag{24}$$

where V_{qs}, i_{qs} are the stator voltage [V] and current [A] (q-axis), V_{ds}, i_{ds} are the stator voltage [V] and current [A] (d-axis), V'_{qr}, i'_{qr} are the rotor voltage [V] and current [A] (q-axis), V'_{dr}, i'_{dr} are the rotor voltage [V] and current [A] (d-axis), ϕ_{qs}, ϕ_{ds} are the stator fluxes [Vs], ϕ'_{qr}, ϕ'_{dr} are the rotor fluxes [Vs], R_s, L_{ls} are the stator dissipation resistance and inductance, R'_r, L'_{lr} are the resistance and inductance of the rotor dissipation, L_s, L'_r are the total inductance of the stator and rotor, L_m is the mutual inductance, ω_e is the electrical angular velocity [rad/s], ω_r is the rotor angular velocity [rad/s], p is the number of pairs of poles.

The mechanical part of the engine description, which is most relevant from the point of view of the modeled stand, is presented in the form of the relationship

$$\frac{\mathrm{d}}{\mathrm{d}t}\omega_r = \frac{T_e - F\omega_r - T_m}{J_s}, \tag{25}$$

where T_e is the electromagnetic torque [Nm], F is the coefficient of viscous friction [Nms], T_m is the mechanical torque on the shaft [Nm], J_s is the rotor and the driven machine moment of inertia [kg·m^2].

To bring the model closer to the test stand, the mechanical-electrical model of the motor was supplemented with a power supply section that included a frequency converter operating based on pulses width modulation.

The use of the mechanical-electrical description in this form, assuming a symmetrical three-phase winding of the stator and rotor and ignoring the saturation of the magnetic circuit of the motor, power losses in the core of the electromagnetic circuit, and the effect of groove effects allows obtaining the most important information about the operation of the motor from the point of view of its mechanical effect on the driven system, which, on the one hand, guarantees results much closer to real, on the other hand, does not contribute to a significant increase in the cost of calculating parameters that are not needed from the point of view of the application of the developed model. The assumption made at the stage of implementing the engine model into the rest of the system was to conduct calculations assuming a fully operational engine. Simulation of damage was assumed only in terms of the mechanical part of the system (especially simulation of local damage in the gears). As a result of the numerous simulations carried out, it turned out that if the analyses of the relevant signals acquired during steady-state operation, or, more precisely, after the completed start-up of the stand, the results from both the mechanical model and the mechanical-electrical model are very close to one another, there is no need to use an elaborate description of the phenomena occurring in the engine, and no need to implement even more complicated models, examples of which in various coordinate systems can be found abundantly in the literature.

6. Model verification

The general problem of identifying and tuning models is widely described in the literature (e.g., Bartczuk *et al.*, 2016; Janiszowski and Wnuk, 2016) or with reference to the Wiener model (Janczak and Korbicz, 2019). The process of verifying the model began with determining its parameters on the test stands, including determining the parameters of the gears, measuring tooth pitch deviations, measuring the geometry of the stand elements to determine the masses and moments of inertia required in the model of the elements, and experimentally determining the torsional stiffness of the torsion shaft and tension shafts. To eliminate possible mistakes, measurements were carried out three times for each shaft. In addition, power losses were determined in order to tune the characteristics of the friction coefficient in the mesh; the damping coefficients of vibrations in the mesh and transverse vibrations in the bearings were determined.

During the experimental tests (Fig. 2), the transverse vibration velocities of the gear shafts (measuring points A, D, and F in Fig. 3) were measured in the direction of the mesh force. Also recorded were two reference signals in the form of pulses generated once per rotation of each shaft, and a third reference signal generated once for a full cycle of tooth associations.

Fig. 2. Test stand with measuring instruments and recording equipment.

Measurements were made using a laser vibrometer, acceleration sensors, and a capacitive directional microphone interfaced with a signal analyzer. A logic circuit connected to optoelectronic sensors mounted near the gear shafts was used to generate shaft rotation markers and the tooth association cycle. The signals were recorded on a measurement computer connected to an eight-channel data acquisition card, while the sampling frequency was 78.125 [kHz]. During the measurements, the temperature of the oil in the gear of the test stand was controlled using a universal multimeter, equipped with a temperature-measuring probe. Measurements were carried out under the following conditions: at constant wheel shaft speeds of n_2 =600; 1200; 1800; 2400 [rpm] and for a unit load of $Q = 1.00$ and 2.15 [MPa].

During the implementation of the measurements, the test gear worked as a reducer. The duration of each measurement was 12 [s]. The actual analysis of the recorded signals was carried out in Matlab and started by averaging with the repetition period of the tooth

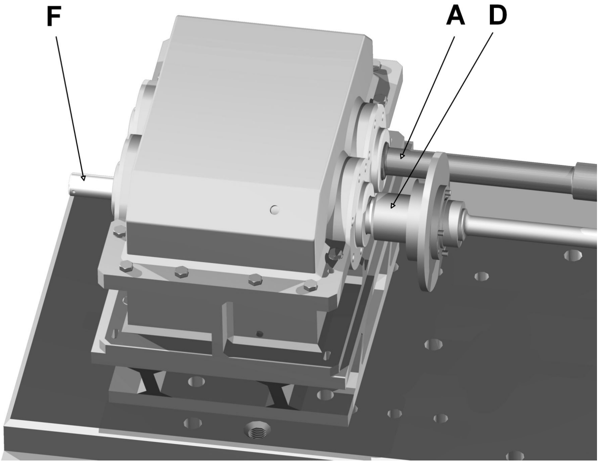

Fig. 3. Location of measurement points on the test gear of the test stand: three points A, D and F as described in Fig. 1 (A: pinion shaft, D and F: wheel shaft).

association cycle. Verification of the model was carried out on two test stands using a total of nine pairs of gears, differing in geometric parameters and deviations of outline and pitch. Among the wheels tested were both straight and helical gears with different tooth line inclination angles.

A comparison of the RMS values and FFT spectra of the transverse vibration velocities in the wheel shaft measured on the test stand and those obtained from the simulation confirmed that the developed model was correctly identified. On this basis, it can be concluded that also the forces in the bearings obtained from the simulation correspond to those in the real gear.

7. Example of using the model for gear design

To illustrate the usefulness of the developed model at the construction stage for optimizing its design, the following will present its use for determining dynamic surplus in the meshing of HCR wheels. Four combinations of geometric parameters of pairs of gears were used. The number of teeth of the pinion was 32, the teeth of the wheel equaled 48, and the module was 2.25 mm. The wheels had a straight mesh, the nominal transverse pressure angle was 20º, and the wheel axis distance was 91.5 mm. Outline displacement coefficients were 0.362 and 0.365 for the pinion and wheel, respectively. It was assumed that the width of the mesh was 20 mm. By appropriately selecting the tooth head height factor in the range of 1.0 to 1.3, the transverse contact ratio was in the range from 1.579 to 2.003. For the wheel pairs used in the calculations, only the condition of the pinion slip of the HCR pair, exceeding the permissible value by less than 2 percent, was not met.

Simulation calculations were performed in the wheel speed range n_2 = 300÷12,000 [rpm]. The speeds were changed with a step of 300 [rpm]. Gear operation was simulated under the unit load Q = 1.5 and 4.0 MPa. In all simulations, the same distribution of tooth pitch deviations with maximum values defined by the 6th class of manufacturing accuracy was assumed.

The vibroactivity of the gear was evaluated by analyzing the values of the mesh force, in the time intervals between the inputs to the meshing of successive pairs of teeth. The dynamic coefficient K_c is determined by the relation

$$K_c = \frac{1}{N} \sum_{j=0}^{N-1} \frac{F_{zdyn}^{max}(t_j : t_{j+1})}{F_{stat}} \, [-], \tag{26}$$

where K_c is the total dynamic factor, N is the number of analyzed intervals, j is the number of analyzed interval, $j = \phi, \dots, N-1$, t_j is the time of entry into the meshing of the next pair of teeth, $F_{zdyn}^{\max}(t_j : t_{j+1})$ is the maximum value of the total dynamic mesh force in the analyzed time interval.

The dynamic surplus values in the analyzed speed range are shown in Fig. 4.

The waveforms of the RMS values of the vibration velocity in the bearings of the pinion shaft (point A: according to Fig. 3) and the wheel (point D) for the load Q = 4.0 are presented in Figs. 5 and 6. Both the values of the dynamic coefficient and the RMS values of the transverse vibration velocity of the pinion and wheel shafts confirm the favorable properties of the high meshing. There is a reduction in the RMS values of the transverse vibration velocities of the shafts over the entire analyzed speed range (the greater the higher the value of the load). For a load of Q = 1.5 [MPa], the differences between the courses of the RMS values are smaller, but the nature of the changes is identical.

8. Summary

Despite many years of intensive development of dynamic models, work on their improvement continues, and they also find further application possibilities. The literature review presented here shows that the models developed today have much greater computational capabilities than their predecessors, which allows this variety of applications to be constantly expanded.

The assumptions for the construction of the models developed by the author of the article, presented in this work and concerning, among others, a three-dimensional method of modeling the mesh with variable stiffness along the meshing section, taking into account the susceptibility of bearings and variable rotational speed and load, as well as the interaction of individual elements of the drive train with each other, allow their use in a wide range of

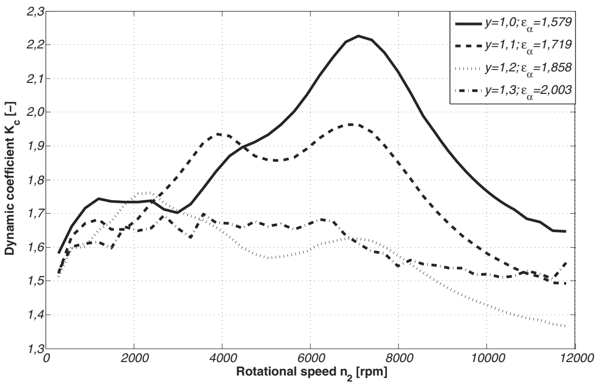

Fig. 4. Influence of tooth head height factor y/values of transverse contact ratio ϵ_α on the total dynamic factor K_c under a load of $Q = 4.0$ [MPa]: gear with pitch deviations, 6th manufacturing accuracy class.

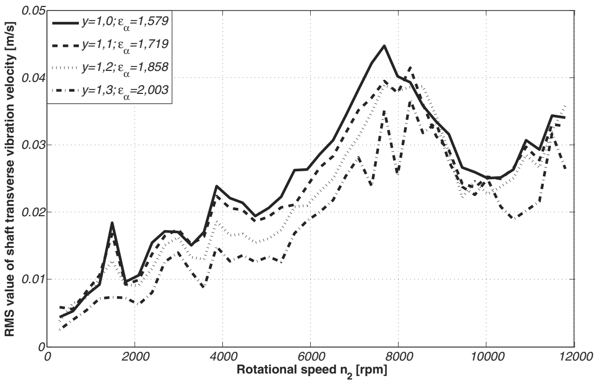

Fig. 5. Effect of tooth head height factor y/values of transverse contact ratio ϵ_α on the RMS values of the transverse vibration velocity of the pinion shaft (point A), load $Q = 4.0$ MPa.

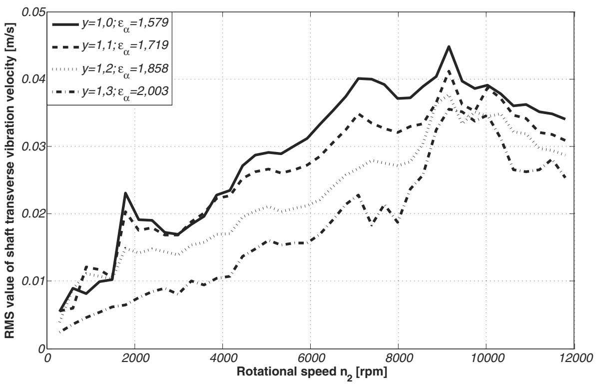

Fig. 6. Effect of tooth head height factor y/values of transverse contact ratio ϵ_α on the RMS values of the transverse vibration velocity of the wheel shaft (point D), load $Q = 4.0$ [MPa].

research. The models known from the literature very often either accurately described the phenomena occurring in the gear with complete disregard for the effects of the power transmission system, or took such effects into account, but were characterized by gross simplifications of the description of phenomena in the gearbox. Many of them were also characterized by simplifications which cannot be justified today, such as constant gear stiffness or two-dimensional analysis of phenomena in the meshings. The description presented here concerns a model of a station with gears operating in a circulating power system. Due to the volume of the article, according to the information in the abstract of the paper, several results obtained from the studies conducted with the model, specific to the gear design stage, and more specifically to the evaluation of the effect of the tooth head height factor and the associated transverse contact ratio on the vibratory activity of the gear determined by the vibration velocities of the pinion and wheel shafts, where presented.

Over a wide range of speeds, the effect of selected design factors on the RMS values of transverse vibration accelerations of the pinion and the wheel shafts was determined. In the same range, the effect of these factors on the values of the total dynamic coefficient, and thus on the values of the forces in the gears related to the static force, was also determined. Although the relationships are known, with the use of the developed program it is possible to determine the exact changes under specific operating conditions. The validation of the model, carried out over a wide range of speeds and loads, taking into account various design parameters of the gears and implemented on two test stands, also allows the simulation results presented in the article to be considered correct, and the model itself to be an effective tool for its purposes.

References

Ajmi, M. and Velex, P. (2005). A model for simulating the quasi-static and dynamic behaviour of solid wide-faced spur and helical gears, *Mechanism and Machine Theory* **40**(2): 173–190.

Al-Tubi, I., Long, H., Zhang, J. and Shaw, B. (2015). Experimental and analytical study of gear micropitting initiation and propagation under varying loading conditions, *Wear* **328–329**: 8–16.

Alves, J.T., Wang, J., Guingand, M., de Vaujany, J.-P. and Velex, P. (2012). Static and dynamic models for spiral bevel gears, *Mechanics & Industry* **13**(5): 325–335.

Bartczuk, Ł., Przybył, A. and Cpałka, K. (2016). A new approach to nonlinear modelling of dynamic systems based on fuzzy rules, *International Journal of Applied Mathematics and Computer Science* **26**(3): 603–621, DOI: 10.1515/amcs-2016-0042.

Bartelmus, W. (2001). Mathematical modelling and computer simulations as an aid to gearbox diagnostics, *Mechanical Systems and Signal Processing* **15**(5): 855–871.

Blankenship, G.W. and Singh, R. (1992). A comparative study of selected gear mesh interface dynamic models, *6th International Power Transmission and Gearing Conference: Advancing Power Transmission into the 21st Century, Scottsdale, USA,* pp. 137–146.

Chen, Z., Zhang, J., Zhai, W., Wang, Y. and Liu, J. (2017). Improved analytical methods for calculation of gear tooth fillet-foundation stiffness with tooth root crack, *Engineering Failure Analysis* **82**: 72–81.

Cheng, C., Wang, M., Wang, J., Shao, J. and Chen, H. (2022). An SFA-HMM performance evaluation method using state difference optimization for running gear systems in high–speed trains, *International Journal of Applied Mathematics and Computer Science* **32**(3): 389–402, DOI: 10.34768/amcs-2022-0028.

Choy, F., Polyshchuk, V., Zakrajsek, J., Handschuh, R. and Townsend, D. (1996). Analysis of the effects of surface pitting and wear on the vibration of a gear transmission system, *Tribology International* **29**(1): 77–83.

Dabrowski, Z., Radkowski, S. and Wilk, A. (2000). *Dynamics of Gears. Research and Simulation in Operationally Oriented Design*, WiZP Institute of Technology Exploitation, Radom, (in Polish). .

Dadon, I., Koren, N., Klein, R. and Bortman, J. (2018). A realistic dynamic model for gear fault diagnosis, *Engineering Failure Analysis* **84**: 77–100.

Ding, H. and Kahraman, A. (2007). Interactions between nonlinear spur gear dynamics and surface wear, *Journal of Sound and Vibration* **307**(3): 662–679.

Ericson, T.M. and Parker, R.G. (2014). Experimental measurement of the effects of torque on the dynamic behavior and system parameters of planetary gears, *Mechanism and Machine Theory* **74**: 370–389.

Fernández, A., Iglesias, M., de Juan, A., García, P., Sancibrián, R. and Viadero, F. (2014). Gear transmission dynamic: Effects of tooth profile deviations and support flexibility, *Applied Acoustics* **77**: 138–149.

Grzadziela, A., Kiciński, R., Szturomski, B. and Piskur, P. (2021). Simulation analysis of the stabilization of the hooks' block with the usage of a wind deflector, *Naše more 2021* **17**: 85.

Grzadziela, A., Kiciński, R., Szturomski, B. and Piskur, P. (2022). Determining the trajectory of the crane block using the finite element method, *Naše more* **69**(2): 92–102.

Gu, X. and Velex, P. (2013). On the dynamic simulation of eccentricity errors in planetary gears, *Mechanism and Machine Theory* **61**: 14–29.

Howard, I., Jia, S. and Wang, J. (2001). The dynamic modelling of a spur gear in mesh including friction and a crack, *Mechanical Systems and Signal Processing* **15**(5): 831–853.

Hydro-Québec/The MathWorks (2009). *SimPowerSystems™ 5 User's Guide*.

Inalpolat, M. and Kahraman, A. (2010). A dynamic model to predict modulation sidebands of a planetary gear set having manufacturing errors, *Journal of Sound and Vibration* **329**(4): 371–393.

Janczak, A. and Korbicz, J. (2019). Two-stage instrumental variables identification of polynomial Wiener systems with invertible nonlinearities, *International Journal of Applied Mathematics and Computer Science* **29**(3): 571–580, DOI: 10.2478/amcs-2019-0042.

Janiszowski, K.B. and Wnuk, P. (2016). Identification of parametric models with *a priori* knowledge of process properties, *International Journal of Applied Mathematics and Computer Science* **26**(4): 767–776, DOI: 10.1515/amcs-2016-0054.

Lai, J., Liu, Y., Xu, X., Li, H., Xu, J., Wang, S. and Guo, W. (2022). Dynamic modeling and analysis of Ravigneaux planetary gear set with unloaded floating ring gear, *Mechanism and Machine Theory* **170**(8): 104696, DOI:10.1016/j.mechmachtheory.2021.104696.

Liang, X., Zuo, M.J. and Hoseini, M.R. (2015). Vibration signal modeling of a planetary gear set for tooth crack detection, *Engineering Failure Analysis* **48**: 185–200.

Ma, H., Pang, X., Feng, R., Zeng, J. and Wen, B. (2015). Improved time-varying mesh stiffness model of cracked spur gears, *Engineering Failure Analysis* **55**: 271–287.

Marques, P.M., Martins, R.C. and Seabra, J.H. (2016). Gear dynamics and power loss, *Tribology International* **97**: 400–411.

Mohammed, O.D., Rantatalo, M. and Aidanpää, J.-O. (2015). Dynamic modelling of a one-stage spur gear system and vibration-based tooth crack detection analysis, *Mechanical Systems and Signal Processing* **54**: 293–305.

Neusser, Z., Vampola, T. and Valasek, M. (2017). Analytical gear mesh model using 3D gear geometry, *Mechanics* **23**(3): 425–431, DOI: 10.5755/j01.mech.23.3.14325.

Osman, T. and Velex, P. (2010). Static and dynamic simulations of mild abrasive wear in wide-faced solid spur and helical gears, *Mechanism and Machine Theory* **45**(6): 911–924.

Özgüven, H.N. and Houser, D. (1988). Mathematical models used in gear dynamics—A review, *Journal of Sound and Vibration* **121**(3): 383–411.

Pandya, Y. and Parey, A. (2013). Simulation of crack propagation in spur gear tooth for different gear parameter and its influence on mesh stiffness, *Engineering Failure Analysis* **30**: 124–137.

Peruń, G. (2006). The effect of damage to the components of a planetary gearbox on the forces in the gears, *Problemy Transportu* **1**(1): 23–38, (in Polish).

Peruń, G. (2017). Modeling of dynamic phenomena occurring in power transmission systems with toothed gears, *Przegląd Mechaniczny* **1**(10): 24–29, (in Polish).

Piskur, P., Szymak, P. and Larzewski, B. (2021). Shipyard crane modeling methods, *Pedagogika* **93**(S6): 279–290.

Razpotnik, M., Bischof, T. and Boltežar, M. (2015). The influence of bearing stiffness on the vibration properties of statically overdetermined gearboxes, *Journal of Sound and Vibration* **351**: 221–235.

Wang, J., Li, R., and Peng, X. (2003). Survey of nonlinear vibration of gear transmission systems, *Applied Mechanics Reviews* **56**(3): 309–329.

Yassine, D., Ahmed, H., Lassaad, W. and Mohamed, H. (2014). Effects of gear mesh fluctuation and defaults on the dynamic behavior of two-stage straight bevel system, *Mechanism and Machine Theory* **82**: 71–86.

Grzegorz Peruń (ORCID: 0000-0003-1549-0383) received his MSc degree in 2004 and his PhD degree in 2010 from the Silesian University of Technology, Katowice, Poland. The thesis, for which he received an award from the Fiat Group (Gliwice/Turyn 2011), was defended with honors. He obtained his habilitation degree at the Air Force Institute of Technology, Warsaw, Poland, in 2018. He is the author and a co-author of over 200 published scientific works, including a monograph, academic textbooks, and two patents. His research interests include mechanical engineering, construction of machines, especially modeling of toothed gears, vibroacoustics, gearbox diagnostic, signal processing, non-destructive testing techniques, GIS, and transport. Since 2019 he has been a professor at the SUT in the Faculty of Transport and Aviation Engineering. He is a member of the Polish Association of Technical Diagnostics (PTDT) and a vice-chairman of the PTDT Audit Committee. He is proficient in several programming languages, which he uses effectively in his academic work and research, and is the author of, among others, software for the resonance defectoscope.

Received: 28 October 2022
Revised: 28 January 2023
Accepted: 6 March 2023